Proceedings of The National Conference
On Undergraduate Research (NCUR) 2013
University of Wisconsin, LaCrosse, WI
April 11-13, 2013

Methods for identifying aerosols by light scattering techniques

Laurel A. Thompson
Departments of Chemistry and Physics
Utah Valley University
800 West University Parkway
Orem, UT 84058 USA

Faculty Advisor: Dr. Timothy E. Doyle

James T. Pearson
Advanced Technology Branch
Test Technology Division
U.S. Army Dugway Proving Ground
Dugway, UT 84022 USA

Abstract

Soldiers and non-combatants are at risk of exposure to dangerous aerosols (airborne particles or droplets) in the form of biological agents such as bacteria, toxins, or viruses. Optical methods provide the option of determining more of the physical properties of aerosols than the current method of detection, which is a moist swath which turns dark upon contact with a biological aerosol. Many systems have been developed for optically measuring particle properties. However, they are usually used from within the aerosol cloud itself. The desired solution is a system that can employ remote sensing to measure aerosol properties from a distance. Standoff detection methods allow a much larger area to be measured at once, providing a more general or big-picture view of the aerosols in a given area. There are several ways that standoff optical scattering data can be analyzed for determining aerosol properties. Using Mie Scattering theory as a basis, we worked, first, to develop a forward modeling system which modeled spectra of aerosols of known size and composition. Next, we set about to solve the reverse problem—determining aerosol properties from the light signals (spectra) using inverse Mie theory—which is difficult because different combinations of aerosol properties can result in similar spectra. The size distribution, however, has a large effect on the optical signal and may therefore be used to differentiate aerosols. The refractive index also contributes to distinct optical spectra. Our hypothesis was that these factors would be sufficient to classify aerosols for risk assessment. We investigated three analytical methods to test this hypothesis: Mie inversion with matrix solutions, empirical curve fitting with polynomial functions, and principal component analysis (PCA). A range of particle sizes and compositions were illuminated by a balanced deuterium/halogen light source and spectral measurements from 200-1100 nm were taken. Optical data over a 200-1300 nm range were also collected from a variety of bio-aerosols using an open path remote sensing system at a 30-meter standoff distance. Mie inversion provided results that matched the experimental data poorly because of matrix singularities. Empirical curve fitting, however, provided results that were highly sensitive to aerosol size and composition, and provided a good method to smooth the data and classify the curvature based on a set of polynomial coefficients. PCA provided a method for grouping the spectra according to their properties. When combined with a modeled database of spectra with inputs of various sizes and size-distributions, our experimental spectra clustered as predicted, according to the size and size distribution found in the experimental aerosols as well.

Keywords: Aerosols, light scattering, inverse methods

1. Introduction

Mie theory predicts the scattering of light from small particles as a function of the particle's size, the particle's refractive index, and the wavelength of light. When integrated over an ensemble of particles suspended in the air (aerosols), the result is the extinction spectrum of the aerosols as a function of the aerosol refractive index and size distribution. This is a direct computation that is known as the "forward" problem, and the known quantities of aerosol refractive index and size distribution are used to model the extinction spectrum as the unknown result. However, in the real world the size distribution and refractive index of the aerosol are usually unknown quantities, and the extinction spectrum is the signal obtained by optical instruments. Work is therefore ongoing to find satisfactory inverse methods for Mie theory to obtain aerosol size distribution and refractive index.

Inverse solutions to Mie theory have been investigated for a variety of measurement configurations. Inverse methods for backscatter measurements of aerosols using broad bandwidth, multi-wavelength, and micro-pulse lidars in the infrared (IR) spectral region have been studied,[1-3] as well as open-path Fourier transform infrared (OP-FTIR) spectral measurements of water droplets in the atmosphere.[4]

In addition to developing a functional inverse method, it is also critical that the optical measurements are in a spectral region that is sensitive to bioaerosols. Although a study in 2000 concluded that bioaerosols will not have characteristic spectral signatures to differentiate them from naturally occurring fog, their calculations were limited to the 8-12 μm IR band.[5] In contrast, measured transmission spectra of microorganisms in the UV-Vis spectral region of 200-900 nm provided characteristic signatures that allowed the differentiation of *Escherichia coli*, *Pantoea agglomerans*, *Bacillus subtilis* spores, and *Bacillus globigii* spores.[6] Calculations show that the Vis-NIR spectral band at 400-1200 nm is also useful for measuring nonspherical particles such as *Bacillus subtilis* spores.[7]

The objective of this project was to develop software for the modeling and analysis of open-path spectral measurements in the UV-Vis-NIR region (200-1100 nm) for the sizing of aerosols of biological and nonbiological origin in the 0.5-5.0 μm size range. Forward models were developed based on Mie scattering theory to calculate extinction spectra of aerosols of a given mean size, size distribution, and complex index of refraction.

2. Methods

A database of measured complex refractive index of hydrosols, representative mineral aerosols, and aerosols of biological origin (bacteria, spores, etc.) was compiled to accurately model the extinction spectra (Table 1). The model spectra, based on Mie scattering theory, were then compared with experimental spectra and used in the development of inverse methods. Inverse methods, based on empirical curve fitting, direct Mie inversion of the Fredholm integral equation, and principal component analysis (PCA) were developed and tested with model, experimental laboratory, and experimental field spectra.

Optical spectra of microparticles suspended in methanol were collected at the Dugway Proving Ground to be used as a model system for studying the optical scattering properties of aerosols. These spectra were used to develop two of the three inverse data analysis approaches: empirical curve fitting and principal component analysis.

Forward models were conducted as illustrated in Figure 1. The complex refractive indices of the aerosol types listed in Table 1 were used to define in the Mie scattering coefficients e_N and f_N which are derived from the Mie theory of electromagnetic wave scattering from a sphere.[8,9] These coefficients were subsequently used to derive the extinction efficiency Q_{ext}:

$$Q_{ext} = \frac{C_{ext}}{\pi a^2} = \frac{2}{(ka)^2} \sum_{N=1}^{\infty} (2N+1)\,\mathrm{Re}\left(e_N + f_N\right) \qquad (1)$$

where N is the order of the series expansion, a is the radius of the sphere, k is the wave vector, and C_{ext} is the extinction cross section. Equation (1) was then used in the Fredholm integral equation to provide the aerosol extinction coefficient $\gamma(\lambda)$:[8,9]

$$\gamma(\lambda) = \int_0^\infty Q_{ext}(a, \lambda, \eta) N(a) \pi a^2 da \,. \quad (2)$$

In Equation (2), $N(a)$ is the log-normal size distribution given in References 10-12 and others.

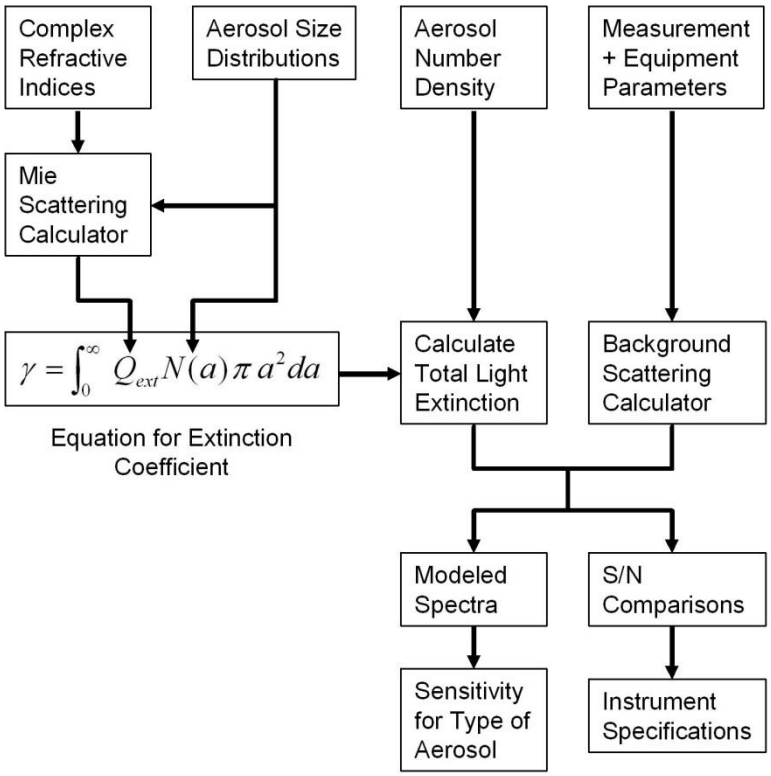

Figure 1. Aerosol scattering algorithm and flowchart for forward scattering model.

Table 1. Aerosol types having reported experimental measurements for the complex refractive index $\eta = \sqrt{\varepsilon / \mu}$.

Aerosol Type	References
Aluminum oxide, alumina (Al2O3)	13
Calcium carbonate, calcite (CaCO3)	14-16
Kaolin, kaolinite (clay mineral)	17
Montmorillonite (clay mineral)	17
Illite (clay mineral)	17
Silicon dioxide, quartz (SiO2)	18
Bacillus subtilis spores (BG)	19
Erwinia herbicola bacteria (EH)	20
Ovalbumin (OV)	21
Water (H20)	22

Initial testing of the forward model was performed using mineral-based aerosols such as aluminum oxide (Al_2O_3) and kaolin, as well as other aerosol types such as borosilicate glass and polystyrene microbeads suspended in methanol. Spectra collected at Dugway were sent to Utah Valley University for analysis. Some sample results are

illustrated in Figure 2. The microparticle spectra were normalized by dividing the signal spectra by the corresponding control spectra.

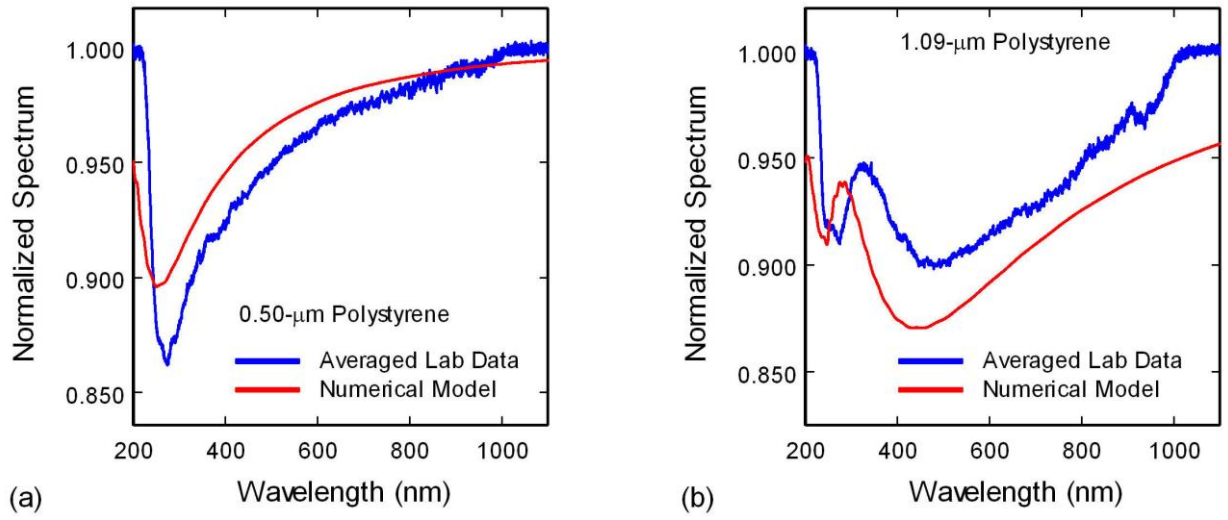

Figure 2. Normalized spectra of methanol with 0.5-μm (a) and 1.09-μm (b) polystyrene microparticles. The blue curves are experimental data and the red curves are results from forward numerical modeling.

Discretization of Equation (2) for computer solution yields a matrix equation of the form $\mathbf{Q} \cdot \mathbf{X} = \boldsymbol{\gamma}$. Inverse methods attempt to solve this equation for the unknown set of aerosol properties symbolized by **X**, primarily the aerosol size distribution and refractive index.

Direct Mie inversion used an iterative method to solve for **X** which involved discretizing the matrix and using Q_{ext} as the weighing factor for the *m*-th projection and *n*-th pixel in a tomography-like fashion, making an initial guess for **X**, and then iteratively calculating corrections to **X**. These types of methods are known as algebraic reconstruction techniques (ART) in tomography.[23,24] In particular, the iterative ART method known as partially constrained ART (PCART) was used in this study.

Curve-fitting created a square matrix from sample points by selecting ten equally spaced points on each experimental spectrum and then fitting them with a ninth-order polynomial using a system of linear equations. The coefficients of the polynomials were then empirically analyzed to provide a method to estimate aerosol type and size distribution.

Principal component analysis (PCA) used an automated comparative program in which a matrix of M wavelengths and N spectra (or trials) was input into a MATLAB program. A column vector matrix was then created from the average of each row. This column is repeated (tiled) onto a new "mean" matrix, $\mathbf{A}_{MxN}$, with the same original number N columns. The mean matrix **A** was then subtracted from the original data matrix **D** to yield a variance matrix $\mathbf{V}_{MxN}$. A MATLAB system command called Singular Value Decomposition was then performed on the transpose of matrix **V**, resulting in a set of three new matrices designated **U**, **S** and **P**: [$\mathbf{U}_{NxN}$, $\mathbf{S}_{NxM}$, $\mathbf{P}_{MxM}$]. **S** stands for signal. The first two rows of matrix **S** are graphed against each other for a scatter chart designating principal component variances.

The PCA method was tested with model extinction spectra calculated for aluminum oxide aerosols having 14 mean sizes (0.25, 0.5, 1.0, 1.5, 2.0, 2.5, 3.0, 4.0, 5.0, 6.0, 7.0, 8.0, 9.0, and 10.0 μm) and 5 size distribution widths (1.5, 1.6, 1.7, 1.8, and 1.9 μm). Field data were also included in the PCA test, consisting of 20 extinction spectra from an equal number of aerosol test runs and a range of aerosol types including kaolin and *Bacillus subtilis* spores (BG). Since the field data was exceptionally noisy, it was first smoothed with a low-pass filter.

3. Results

Direct Mie inversion, accomplished by iterative means, returned poorly fit models, due to ill-conditioned matrices (Figure 3). *Curve Fitting* provided a set of coefficients by which to classify a spectrum. It resulted in a curve that

was similar to the experimental spectrum, but model-like in character (Figure 4), which may be useful if noise is a large problem in future classification and pattern recognition programs. It was used with success in the principal component analysis to check against clustering based on noise.

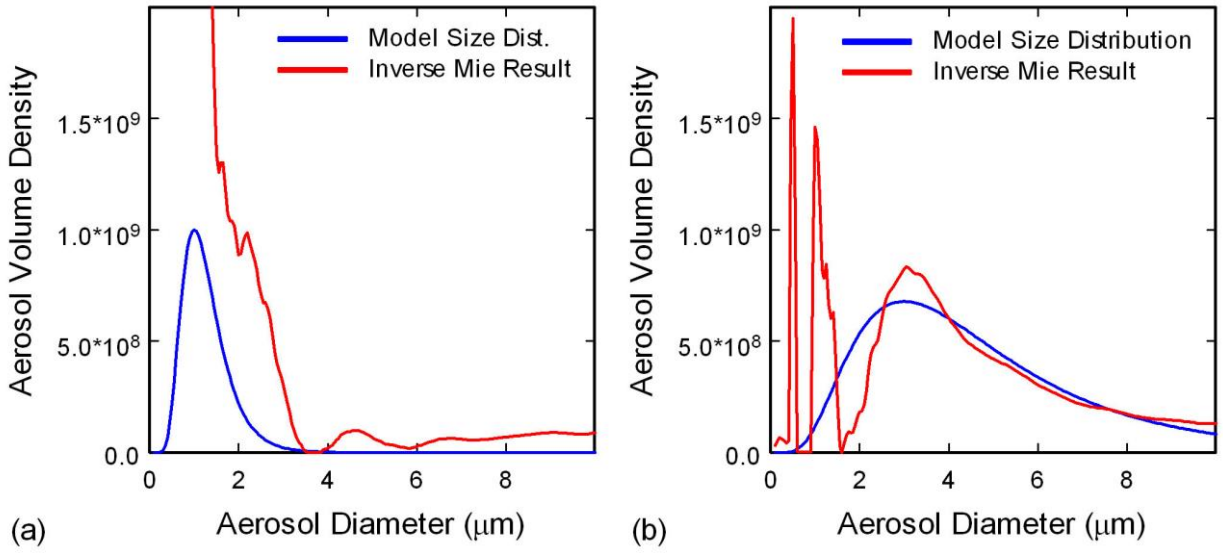

Figure 3. Direct Mie inversion using the iterative PCART tomographic method for aerosols with a BG-spore size distribution (a) and a mineral-dust size distribution (b). Inverse Mie results based on a flat initial condition (constant aerosol density values with size) and a relaxation parameter of $R = 0.001$.

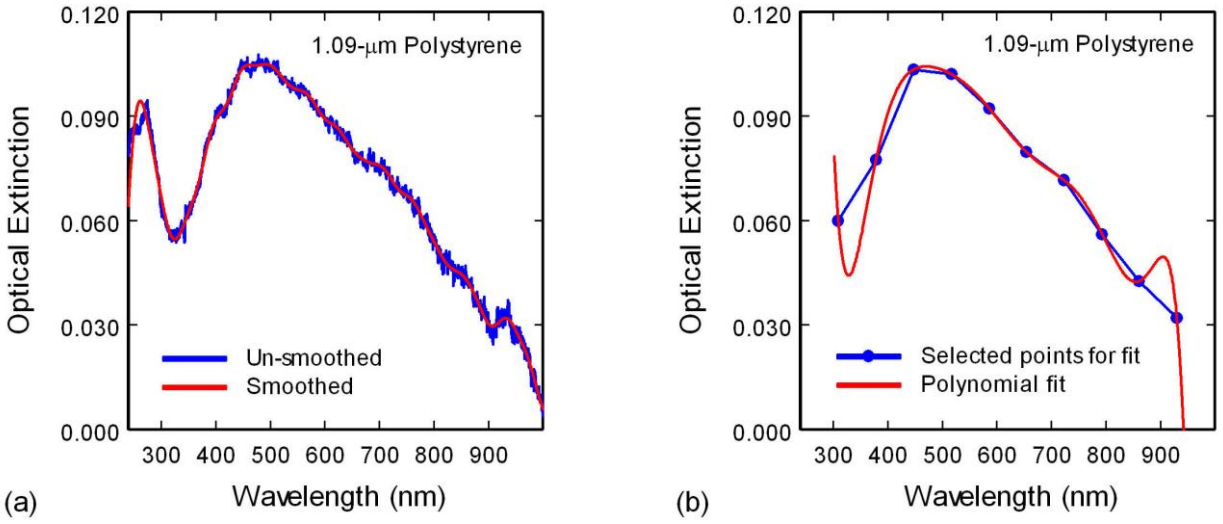

Figure 4. Laboratory extinction spectra of 1.09-μm diameter polystyrene microparticles suspended in methanol. (a) Extinction spectra showing original experimental data (blue curve) and smoothed data (red curve). (b) Selected points for curve fitting (blue curve) and resulting ninth-order polynomial fit (red curve).

Figure 5 is a cluster plot displaying the first two principal component scores of the model aerosol data with the curve-fit results from the experimental spectra (field data). The plot of the model data shows a distinctive arc pattern, with 14 sub-arcs corresponding to 14 mean particle sizes, where the five size distributions (wide to narrow) are the five points within each sub-arc cluster. The sub-arc at the farthest left of the arc are the smallest size aerosols, and each sub-arc moving across the arc to the right corresponds to a progressively larger size.

Additionally, the model data points on the outer edge of the arc correspond to the smallest distribution width, with the width increasing to the inside of the arc. This indicates that the mean size of the experimental aerosols was below 0.25 μm and that their size distribution widths were greater than 1.9 μm. Data from Dugway's automated particle sizing system (APS) appear to confirm this conclusion.

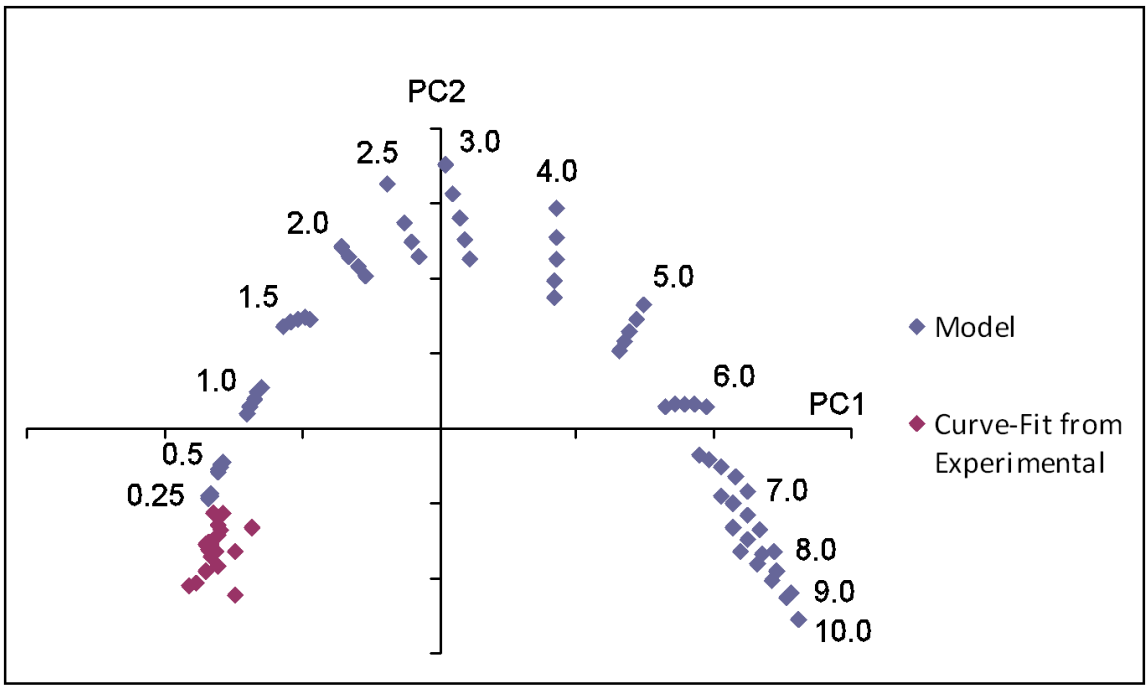

Figure 5. PCA cluster plot of modeled aluminum oxide aerosols (model) and field data (experimental) comprised of open-path spectral measurements from the U.S. Army Dugway Proving Ground. Displayed numbers are the aerosol mean size in micrometers.

4. Discussion and Future Directions

The principal component analysis approach was most encouraging, especially because it was a blind study, with investigation of the experimental particle sizing completed after configuration of the forward model array. With or without the curve-fitting, the experimental data clustered at the same spot in comparison to the model data, which suggests that for this particular situation, the curve-fitting was not necessary and current smoothing models are sufficient to eliminate noise in this experiment.

Of the three methods studied in this project for obtaining aerosol size distributions from open-path spectral measurements in the UV-Vis-NIR region, PCA was found to be the fastest, easiest to interpret, and the most capable of resolving mean aerosol size and size distribution width. Surprisingly, although many of the extinction spectra for aluminum oxide are difficult to differentiate upon direct inspection, the principal component scores are well resolved in the cluster plot shown in Figure 5. This ability to resolve aerosol size and distribution width is remarkable, and demonstrates that PCA is a powerful method for analyzing open-path aerosol measurements in the UV-Vis-NIR region.

Although the field data in Figure 5 are in the lower left corner of the cluster arc, this result is consistent with the aerosol size distributions measured by independent aerosol counting instruments. These distributions are typically weighted towards the smallest aerosol sizes. Additionally, these distributions were not always a log-normal size distribution, which may skew their PCA scores. The aerosol type (refractive index) may also be contributing to the offset in the PCA scores, as the models were all based on aluminum oxide's refractive index.

Although empirical curve fitting was able to provide a unique set of coefficients for each laboratory spectrum, more work is needed to understand how these coefficients relate to aerosol type (refractive index), mean aerosol size, and aerosol size distribution.

Direct Mie inversion proved to be the least successful approach in this study, due primarily to the ubiquitous problem that the extinction efficiency matrix is ill-conditioned. The results from this study indicate that exact inversion methods will not work, but that iterative methods might work for an approach that uses a range of log-normal distributions for initial conditions and solution fitness criteria to select the best solution. It may be that PCA or other pattern recognition programs could be a key to accomplishing this.

5. Conclusion

Computer programs were developed to simulate and analyze open-path spectral measurements of aerosols in the UV-Vis-NIR region (200-1100 nm) and obtain information on aerosol size, size distribution, and composition. Aerosols of interest included mineral-based dusts and those of microbiological origin such as bacteria and complex proteins. A library of the complex refractive indices for the aerosol compositions was compiled from published measurements for use in the computer programs. Forward models were developed that used Mie scattering theory to calculate aerosol extinction cross sections, coefficients, and spectra from the aerosol's complex refractive index and size distribution. The modeled spectra showed which wavelength regions will be most sensitive to specific aerosol sizes and size distribution widths, and were used for the development of inverse methods.

Three inverse methods were investigated for effectiveness in determining aerosol size, size distribution, and composition. These methods were empirical curve fitting of the measured spectra using high-order polynomial curve fits, direct Mie inversion of the Fredholm integral equation, and principal component analysis (PCA) of the spectral measurements using model spectra from the forward models as a comparative database. Both laboratory and field data were used to develop and test the above inverse methods. The most successful of the three methods was PCA. PCA provided the greatest resolution distinguishing size and size distribution from aerosol measurements in the size range of interest (0.5-5.0 μm). PCA was also the easiest method to implement and interpret. PCA, combined with a forward model database and curve fitting of measured spectra, was found to be an exceptionally powerful approach to classifying aerosol characteristics from spectral data. The primary conclusion from this study is that the PCA method will be an exceptionally important approach for determining aerosol sizes and size distributions from open-path spectral measurements, and may have potential for even finer discrimination of aerosol types based on refractive index.

6. Acknowledgments

The author wishes to express her appreciation to the U.S. Army Dugway Proving Ground for providing the funding and experimental data for this project.

7. References

1. Gillespie, J. B., Ligon D. L., Pellegrino, P. M., and Fell, N. F., Jr. (**2001**). "Broad Bandwidth Lidar for Standoff Bioaerosol Size Distribution," (U.S. Army Research Laboratory, Adelphi, MD).
2. Varma, R. M., Hashmonay1, R. A., Du, K., Rood, M. J., Kim, B. J., and Kemme, M. R. (**2008**). "A Novel Method to Quantify Fugitive Dust Emissions Using Optical Remote Sensing," in *Advanced Environmental Monitoring.* (Springer Netherlands, New York) 143-154.
3. Du, K., Rood, M. J., Welton, E. J., Varma, R. M., Hashmonay, R. A., Kim, B. J., and Kemme, M. R. (**2011**). "Optical remote sensing to quantify fugitive particulate mass emissions from stationary short-term and mobile continuous sources: Part I. Method and examples," Environ. Sci. Technol. **45**, 658-665.
4. Hashmonay, R. A. and Yost, M. C. (**1999**). "On the application of open-path Fourier transform infra-red spectroscopy to measure aerosols: Observations of water droplets," Environ. Sci. Technol. **33**, 1141-1144.
5. Ligon, D. A., Wetmore, A., Gillespie, P. (**2000**). "Spectral Signatures of Bioaerosol Clouds using WAVES," (U.S. Army Research Laboratory, Adelphi, MD).

6. Alupoaei, C. E., Olivares, J. A. Garcia-Rubio, L. H. (**2004**). **"**Quantitative spectroscopy analysis of prokaryotic cells: vegetative cells and spores," Biosens. Bioelectron. **19**, 893-903.
7. Velazco-Roa, M. A., Dzhongova, E., and Thennadil, S.N. (**2008**). "Complex refractive index of nonspherical particles in the visible near infrared region—application to *Bacillus subtilis* spores," Appl. Opt. **47**:33, 6183-6189.
8. van de Hulst, H. C. (**1981**). *Light Scattering by Small Particles* (John Wiley and Sons, Inc., New York, 1957; Dover, New York).
9. Bohren, C. F., and Huffman, D. R. (**1998**). *Absorption and Scattering of Light by Small Particles* (John Wiley & Sons, Inc., New York, 1983; Wiley Professional Paperback Edition).
10. von Salzen, K. (**2006**). "Piecewise log-normal approximation of size distributions for aerosol modeling," Atmos. Chem. Phys., 6, 1351–1372.
11. Kobayashi, H., Arao, K., Murayama, T., Iokibe, K., Koga, R., and Shiobara, M. (**2007**). "High-resolution measurement of size distributions of Asian dust using a Coulter multisizer," J. Atmos. Oceanic Tech. **24**, 194-205.
12. Howard, A. Q. (**2010**). "Open Path Aerosol Particle Sizing in the 0.5 to 5 μm Diameter Range," (Energy Dynamics Laboratory, Utah State University, September 9, 2010).
13. Koike, C., Kaito, C., Yamamoto, T., Shibai, H., Kimura, S., and Suto, H. (**1995**). "Extinction spectra of corundum in the wavelengths from UV to FIR," Icarus **114,** 203-214.
14. Marra, A. C., Politia, R., Blancoa, A., Brunettoa, R., Fontia, S., Marzoa, G. A., and Orofino, V. (**2006**). "Optical constants of particulate minerals from reflectance measurements: The case of calcite," J. Quant. Spectrosc. Radiat. Transfer. **100**, 250-255.
15. Thompson, D. W., DeVries, M. J., Tiwald, T. E., and Woollam, J. A. (**1998**). "Determination of optical anisotropy in calcite from ultraviolet to mid-infrared by generalized ellipsometry," Thin Solid Films **313-314,** 341-346.
16. Vincent, R. K. (**1972**). "Emission polarization study on quartz and calcite," Appl. Opt. **11**:9, 1942-1945.
17. Egan, W. G. and Hilgeman, T. W. (**1979**). "Complex refractive index of clay minerals," in *Optical Properties of Inhomogeneous Materials* (Academic Press, New York).
18. Khashan, M. A., and Nassif, A. Y. (**2001**). "Dispersion of the optical constants of quartz and polymethyl methacrylate glasses in a wide spectral range: 0.2-3 μm," Opt. Commun. **188,** 129-139.
19. Tuminello, P. S., Arakawa, E. T., Khare, B. N., Wrobel, J. M., Querry, M. R., and Milham, M. E. (**1997**). "Optical properties of *Bacillus subtilis* spores from 0.2 to 2.5 μm," Appl. Opt. **36**:13, 2818-2824.
20. Arakawa, E. T., Tuminello, P. S., Khare, B. N., and Milham, M. E. (**2003**). "Optical properties of *Erwinia herbicola* bacteria at 0.190–2.50 μm," Biopolymers (Biospectroscopy) **72,** 391-398.
21. Arakawa, E. T., Tuminello, P. S., Khare, B. N., and Milham, M. E. (**2001**). "Optical properties of ovalbumin in 0.130–2.50 μm spectral region," Biopolymers (Biospectroscopy) **62,** 122-128.
22. Segelstein, D. (**1981**). "The Complex Refractive Index of Water," M.S. Thesis, University of Missouri, Kansas City, Missouri.
23. Kaczmarz, S. (**1937**). "Angenäherte auflösung von systemen linearer gleichungen," Bulletin International De L' Académie Polonaise des Sciences et Lettres **3**, Class A, 355-357.
24. Gordon, R., Bender, R., and Herman, G. T. (**1970**). "Algebraic Reconstruction Techniques (ART) for three-dimensional electron microscopy and x-ray photography," J. Theor. Biol. **29**, 471-476.